

# Modeling of A Multilevel Voltage Source Converter using the Fast Time-Domain Method

R. K. Subroto and K. L. Lian *Member, IEEE*,

**Abstract**—Power system harmonics can increase system losses, excite resonant frequency, and cause equipment damage. It is therefore essential to develop accurate harmonic models for harmonic sources such as power converters. During last decades, renewable energy sources have become an important part of the worldwide concern with clean power generation. In response to the growing demand for medium and high power trends, multilevel converters (MCs) have been attracting growing considerations. As they become more spread-out, their harmonic impact on the system could be significant. In this paper, a fast time-domain method (FTDM) suitable for modeling a MC is proposed. The FTDM essentially model the harmonic of interest as a harmonic state and solve it together with the system differential equations. Since the solution is analytical, the FTDM is very accurate. Nevertheless, to model a MC, the FTDM requires to solve a very large exponential matrix. Hence, a Krylov subspace method is proposed to solve for the exponential matrix, resulted from the FTDM. Two case studies on two different modulations (in-phase disposition and phase-shifted modulations) are performed to validate the proposed method. As demonstrated in the paper, the computation time of the proposed method is much shorter compared to the brute-force time-domain simulators such as PSCAD/EMTDC. Moreover, when compared to other solvers, the proposed Krylov-based method yields the best in terms of calculation time.

**Index Terms**—Multilevel converters, time-domain method, Steady-state analysis, Krylov subspace method, Harmonic Analysis

## I. INTRODUCTION

During last decades, renewable energy sources have become an important part of the worldwide concern with clean power generation. However, due to their intermittent nature, power electronic converters are generally required for them to connect to the grid. In response to the growing demand for medium and high power trends, multilevel converters (MCs) have been attracting growing considerations. They enable the output voltage to be raised without increasing the voltage rating of switching components so that direct connection to the grid is possible without the use of expensive and bulky transformers. In addition, compared to the conventional two-level converters, they have lower common mode voltage, lower voltage stress on power switches, lower dv/dt ratio, and better harmonic content. Thus, they have also been applied in a wide range of industrial applications such as textile and paper industry, steel mills, and railway traction [1]. As they become more spread-out, their harmonic impact on the system could be significant. It is therefore essential to develop accurate harmonic models of these converter in order to predict

how harmonics propagate through the system and to quantify the distortion in voltage and current waveforms at various locations in power network. There have been many research papers addressing harmonic modeling of a two-level converter. However, only a few papers dealing with harmonic models of MCs. Thus, the goal of this paper is to develop an accurate and computation efficient harmonic model of MCs.

In this paper, a fast time-domain method (FTDM) suitable for modeling a cascaded MC (CMC) is proposed. Since the presentation of the CMC in 1975, the converter has received much research attention due to its advantages compared to other MC topologies in terms of simplicity, modularity, and the number of voltage level with a minimum number of power semiconductor devices. Moreover, a CMC synthesizes a desired voltage from several separate dc sources, which may be obtained from the energy storages such as batteries, fuel cells and renewable energy sources such as Photovoltaic systems. Finally, other MC topologies such as MMC have been developed as a derivative of the CMC cells.

The FTDM was first proposed by Lehn [2], and has been applied to solve for a conventional three-phase two-level voltage source converter (VSC). The FTDM essentially model the harmonic of interest as a harmonic state and solve it together with the system differential equations. Since the solution is analytic, the FTDM is very accurate as compared to brute force time-domain method and frequency domain method, which are limited by Nyquist criterion and Gibbs phenomena, respectively. Nevertheless, to model a MC, the FTDM requires to solve a very large exponential matrix. Hence, modification is needed in the original FTDM in order to model the CMCs. In this paper, we proposed to use Krylov subspace method [3] to solve for the exponential matrix, resulted from the FTDM. Krylov subspace methods have been applied to formulate power flow problem, reduce order of system, and decrease the solution time of an electromagnetic circuit solver. As demonstrated in this paper and [4], the computation time of the proposed method is much shorter compared to the brute-force time-domain simulators such as PSCAD/EMTDC. Moreover, when compared to the solvers based on Scaling and Squaring (S & S), Padè approximation (PA) [5], and the Matlab expm function (expm), the proposed Krylov-based method yields the shortest in terms of calculation time.

The rest of the paper is organized as follows: Section II describes the state space model of a CMC for  $m$ -cells of H-bridges. Then, we will describe how Krylov subspace method is used to solve the differential equations in Section III. In Section IV, a brief introduction to the PWM strategies used in the paper is described. In Section V, example cases studies are presented. The results are verified with those of

PSCAD/EMTDC, demonstrating the validity of the proposed where method. Finally, a conclusion is given in Section VI.

## II. STATE-SPACE DIFFERENTIAL EQUATIONS FOR CMC

Without loss of generality, the differential equations of CMC with H-bridge cells are derived. The voltage levels,  $l$  in a CMC with H-bridge cells can be found from

$$l = 2m + 1 \quad (1)$$

where  $m$  is the number of H-bridge cells per phase leg. Note that  $l$  is always an odd number for the Cascaded H-Bridge. Fig. 1 shows the corresponding schematic diagram, where each cell is composed of two active switches and a dc voltage source or a capacitor. To simplify the derivation, a simple dc voltage source is used in the figure. Moreover, if the IGBT or GTO switches are assumed to be ideal, only the switching functions of the upper leg pair,  $(S_{a2k-1}, S_{a2k})$ ,  $(S_{b2k-1}, S_{b2k})$ , and  $(S_{c2k-1}, S_{c2k})$  from each cell are needed for modeling the VSC. Note that  $k = 1, \dots, m$ .

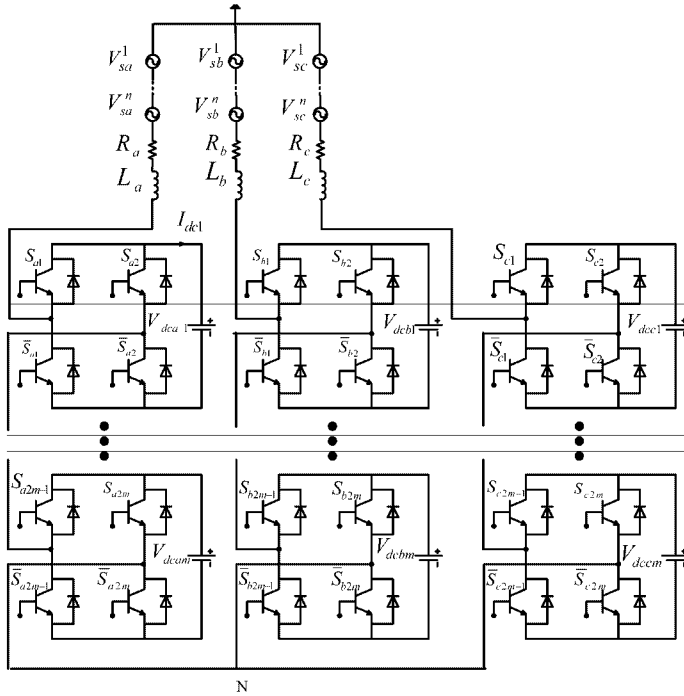


Fig. 1. Schematic diagram of a CMC

Instead of writing the differential equations in the form of  $\dot{\mathbf{x}} = \mathbf{A}\mathbf{x} + \mathbf{B}\mathbf{u}$ , an equivalent homogenous equation in the form of (2) is desired because the convolution integral can be avoided [6]. Note that  $\mathbf{A}$  is the system matrix,  $\mathbf{B}$  is the input matrix, and  $\mathbf{\Omega}$  represents the system matrix of a harmonic oscillator. Moreover, it is much easier to modify the equations when a module is added in or deleted from the system because only a submatrix of  $\mathbf{A}$ ,  $\mathbf{F}_{abc}$ , which contains switching functions, needs to be modified.

$$\frac{d}{dt} \begin{bmatrix} \mathbf{x} \\ \mathbf{u} \end{bmatrix} = \begin{bmatrix} \mathbf{A} & \mathbf{B} \\ \mathbf{0} & \mathbf{\Omega} \end{bmatrix} \begin{bmatrix} \mathbf{x} \\ \mathbf{u} \end{bmatrix} \quad (2)$$

$$\mathbf{x} = \begin{bmatrix} \mathbf{i}_{abc} & \mathbf{v}_{dc} \end{bmatrix}^T,$$

$$\mathbf{i}_{abc} = \begin{bmatrix} i_a & i_b & i_c \end{bmatrix},$$

$$\mathbf{v}_{dc} = \begin{bmatrix} v_{dca} & v_{dcb} & v_{dcc} \end{bmatrix},$$

$$\mathbf{v}_{dca} = \begin{bmatrix} v_{dca1} & \dots & v_{dcam} \end{bmatrix},$$

$$\mathbf{v}_{dcb} = \begin{bmatrix} v_{dcb1} & \dots & v_{dcbm} \end{bmatrix},$$

$$\mathbf{v}_{dcc} = \begin{bmatrix} v_{dcc1} & \dots & v_{dccm} \end{bmatrix},$$

$$\mathbf{u} = \begin{bmatrix} \mathbf{v}_{sa} & \mathbf{v}_{sb} & \mathbf{v}_{sc} \end{bmatrix}^T,$$

$$\mathbf{v}_{sa} = \begin{bmatrix} v_{sax}^1 & v_{say}^1 & \dots & v_{sax}^n & v_{say}^n \end{bmatrix},$$

$$\mathbf{v}_{sb} = \begin{bmatrix} v_{sbx}^1 & v_{sby}^1 & \dots & v_{sbx}^n & v_{sby}^n \end{bmatrix},$$

$$\mathbf{v}_{sc} = \begin{bmatrix} v_{scx}^1 & v_{scy}^1 & \dots & v_{scx}^n & v_{scy}^n \end{bmatrix},$$

$$\mathbf{A} = \begin{bmatrix} \mathbf{G}_{abc} & \mathbf{F}_{abc} \\ \mathbf{0} & \mathbf{0} \end{bmatrix}_{(3+3m) \times (3+3m)},$$

$$\mathbf{G}_{abc} = \begin{bmatrix} \frac{R_a}{L_a} & 0 & 0 \\ 0 & \frac{R_b}{L_b} & 0 \\ 0 & 0 & \frac{R_c}{L_c} \end{bmatrix}_{3 \times 3},$$

$$\mathbf{F}_{abc} = \begin{bmatrix} \mathbf{F}_{a1} & \mathbf{F}_{b1} & \mathbf{F}_{c1} \\ \mathbf{F}_{a2} & \mathbf{F}_{b2} & \mathbf{F}_{c2} \\ \mathbf{F}_{a3} & \mathbf{F}_{b3} & \mathbf{F}_{c3} \end{bmatrix}_{3 \times 3m}$$

$$\mathbf{F}_{a1} = \begin{bmatrix} -\frac{2(S_{a1} - S_{a2})}{3L_a} & \dots & -\frac{2(S_{a2m-1} - S_{a2m})}{3L_a} \end{bmatrix}_{1 \times m},$$

$$\mathbf{F}_{a2} = \begin{bmatrix} \frac{(S_{a1} - S_{a2})}{3L_a} & \dots & \frac{(S_{a2m-1} - S_{a2m})}{3L_a} \end{bmatrix}_{1 \times m},$$

$$\mathbf{F}_{a3} = \begin{bmatrix} \frac{(S_{a1} - S_{a2})}{3L_a} & \dots & \frac{(S_{a2m-1} - S_{a2m})}{3L_a} \end{bmatrix}_{1 \times m},$$

$$\mathbf{F}_{b1} = \begin{bmatrix} \frac{(S_{b1} - S_{b2})}{3L_b} & \dots & \frac{(S_{b2m-1} - S_{b2m})}{3L_b} \end{bmatrix}_{1 \times m},$$

$$\mathbf{F}_{b2} = \begin{bmatrix} -\frac{2(S_{b1} - S_{b2})}{3L_b} & \dots & -\frac{2(S_{b2m-1} - S_{b2m})}{3L_b} \end{bmatrix}_{1 \times m},$$

$$\mathbf{F}_{b3} = \begin{bmatrix} \frac{(S_{b1} - S_{b2})}{3L_b} & \dots & \frac{(S_{b2m-1} - S_{b2m})}{3L_b} \end{bmatrix}_{1 \times m},$$

$$\mathbf{F}_{c1} = \begin{bmatrix} \frac{(S_{c1} - S_{c2})}{3L_c} & \dots & \frac{(S_{c2m-1} - S_{c2m})}{3L_c} \end{bmatrix}_{1 \times m},$$

$$\mathbf{F}_{c2} = \begin{bmatrix} \frac{(S_{c1} - S_{c2})}{3L_c} & \dots & \frac{(S_{c2m-1} - S_{c2m})}{3L_c} \end{bmatrix}_{1 \times m},$$

$$\mathbf{F}_{c3} = \begin{bmatrix} -\frac{2(S_{c1} - S_{c2})}{3L_c} & \dots & -\frac{2(S_{c2m-1} - S_{c2m})}{3L_c} \end{bmatrix}_{1 \times m},$$

$$\mathbf{B} = \begin{bmatrix} \begin{bmatrix} \frac{1}{L_a} & 0 \\ 0 & 0 \end{bmatrix} & \cdots & \mathbf{0} \\ \vdots & \ddots & \vdots \\ \mathbf{0} & \cdots & \begin{bmatrix} \frac{1}{L_c} & 0 \\ 0 & 0 \end{bmatrix} \end{bmatrix}_{6n \times 6n},$$

$$\mathbf{\Omega} = \begin{bmatrix} \begin{bmatrix} 0 & -\omega \\ \omega & 0 \end{bmatrix} & \cdots & \mathbf{0} \\ \vdots & \ddots & \vdots \\ \mathbf{0} & \cdots & \begin{bmatrix} 0 & -\omega \\ \omega & 0 \end{bmatrix} \end{bmatrix}_{6n \times 6n}$$

The harmonics of interests can then be calculated by the frequency coupling matrix, as demonstrated in [4].

### III. KRYLOV SUBSPACE METHOD

The Krylov subspace methods have been developed in the early 1980's for iteratively solving the linear problem  $\mathbf{G}\mathbf{x} = \mathbf{b}$  for large and sparse  $\mathbf{G}$  matrices [7]. If  $\mathbf{G}$  is nonsymmetric, the usual approach is to minimize the residual in the formulation  $\mathbf{b} - \mathbf{G}\mathbf{y}$ , which has led to the approach of Generalized Minimal Residual (GMRES) method. It was realized that GMRES could be used when the vectors  $e^{\mathbf{G}\mathbf{y}}$ , not  $e^{\mathbf{G}}$  in isolation, is required to be estimated [8] for a given vector  $\mathbf{y}$ .

It is known that  $e^{\mathbf{G}t}\mathbf{y}$  can be expressed using the Taylor expansion

$$e^{\mathbf{G}t}\mathbf{y} = \mathbf{y} + \frac{t\mathbf{G}}{1!}\mathbf{y} + \frac{(t\mathbf{G})^2}{2!}\mathbf{y} + \cdots, \quad (3)$$

where  $\mathbf{G}$  is an  $n \times n$  matrix.

The approximation of (3) can be obtained from a Krylov subspace, which is defined as

$$\mathbf{K}_m = \text{span}\{\mathbf{y}, \mathbf{G}\mathbf{y}, \dots, \mathbf{G}^{m-1}\mathbf{y}\} \quad (4)$$

However, these vectors form a poor basis for the Krylov subspace because they point in almost the same direction as the dominant eigenvector of  $\mathbf{G}$ . Thus, an orthogonal process, which is called the Arnoldi iteration [9], is used to form the orthonormal basis  $\mathbf{Q}_m = \{\mathbf{q}_1, \dots, \mathbf{q}_m\}$ , whose algorithm can be found in [8]. Because of the orthogonality of  $\mathbf{Q}_m$ , the projection matrix of  $\mathbf{G}$  onto the Krylov subspace can be expressed as [8]

$$\mathbf{H}_m = \mathbf{Q}_m^T \mathbf{G} \mathbf{Q}_m. \quad (5)$$

Since  $\mathbf{Q}_m^T \mathbf{Q}_m = \mathbf{I}_m$ ,

$$e^{\mathbf{G}t}\mathbf{y} = \mathbf{Q}_m^T \mathbf{Q}_m e^{\mathbf{G}t}\mathbf{y} \quad (6)$$

Moreover, since  $\mathbf{q}_1 = \frac{\mathbf{y}}{\|\mathbf{y}\|_2}$  and  $\mathbf{q}_j^T \mathbf{y} = 0$  for any  $j > 1$ ,

$$\mathbf{Q}_m^T \mathbf{y} = \|\mathbf{y}\|_2 \mathbf{e}_1, \quad (7)$$

where  $\mathbf{e}_1$  is the first column of  $\mathbf{I}_m$ . Consequently,

$$e^{\mathbf{G}t}\mathbf{y} \approx \|\mathbf{y}\|_2 \mathbf{Q}_m e^{\mathbf{H}_m t} \mathbf{e}_1, \quad (8)$$

$\mathbf{H}_m$  is a Hessenberg matrix which is almost a triangular matrix with zero entries below the first subdiagonal. Moreover, the

size of  $\mathbf{H}_m$  is  $m \times m$ , where  $m$  is much smaller than  $n$ . Thus, the advantage of (8) is that the large sparse  $e^{\mathbf{G}t}$  problem is replaced by a small dense  $e^{\mathbf{H}_m t}$  problem, which effectively reduce the computation time.

### IV. MULTICARRIER PULSE WIDTH MODULATION

There have been many different pulse width modulation strategies proposed for MCs over the past two decades [10]. They include carrier-based modulation scheme, space vector modulation, and selective harmonic elimination method. Among them, the carrier-based modulation strategy is widely used in industry [11]. It is similar to the SPWM strategy for a two-level VSC except for the fact that several carriers are used, and compared with one sinusoidal modulating signal. The number of carriers required to produce  $l$ -level output is  $l - 1$ .

The carrier-based modulation schemes for multilevel converters can be generally classified into two categories [10]: phase-shifted (PS) and level-shifted (LS) modulation. In the PS-PWM modulation, all the triangular carriers have the same frequency and the same peak to peak amplitude, but there is a phase shift between two adjacent carrier waves, given by

$$\phi_{cr} = 360^\circ / (m - 1) \quad (9)$$

The LS-PWM, which is also known as phase-disposition PWM, in general, consists of three-types — in-phase disposition (IPD), alternative phase opposite disposition (APOD), and phase opposite disposition (POD). In this paper, only IPD will be discussed due to its best harmonic profile among the three [12]. IPD-PWM is obtained by comparing the modulating signals with carrier signals which are all in phase [1], [12]. Fig. 2(a) shows the PS-PWM based on unipolar switching scheme [13] whereas Fig. 2(b) shows the IPD-PWM based on bipolar switching scheme [13] for switching frequency ratio,  $m_f = 15$ . These two schemes will be used for the following case studies.

### V. CASE STUDIES

To validate the proposed method, its steady state solutions are compared with those obtained by brute force time domain simulation (PSCAD/EMTDC). The system under study is shown in Fig 1 with the number of the CMC cells equal to three. The values of the parameters are adopted from [14], and listed in TABLE I. A simulation time step of  $10 \mu s$  is chosen for PSCAD/EMTDC to limit integration error. In the following subsections the multilevel VSC is studied under both balanced and unbalanced operating conditions.

#### A. Case 1: Balanced Condition

The multilevel VSC is assumed to connect to a balanced three-phase system, with system voltages given by

$$\begin{aligned} v_{sa}(t) &= v_s \cos(\omega t) \\ v_{sb}(t) &= v_s \cos\left(\omega t + \frac{2\pi}{3}\right) \\ v_{sc}(t) &= v_s \cos\left(\omega t + \frac{4\pi}{3}\right), \end{aligned}$$

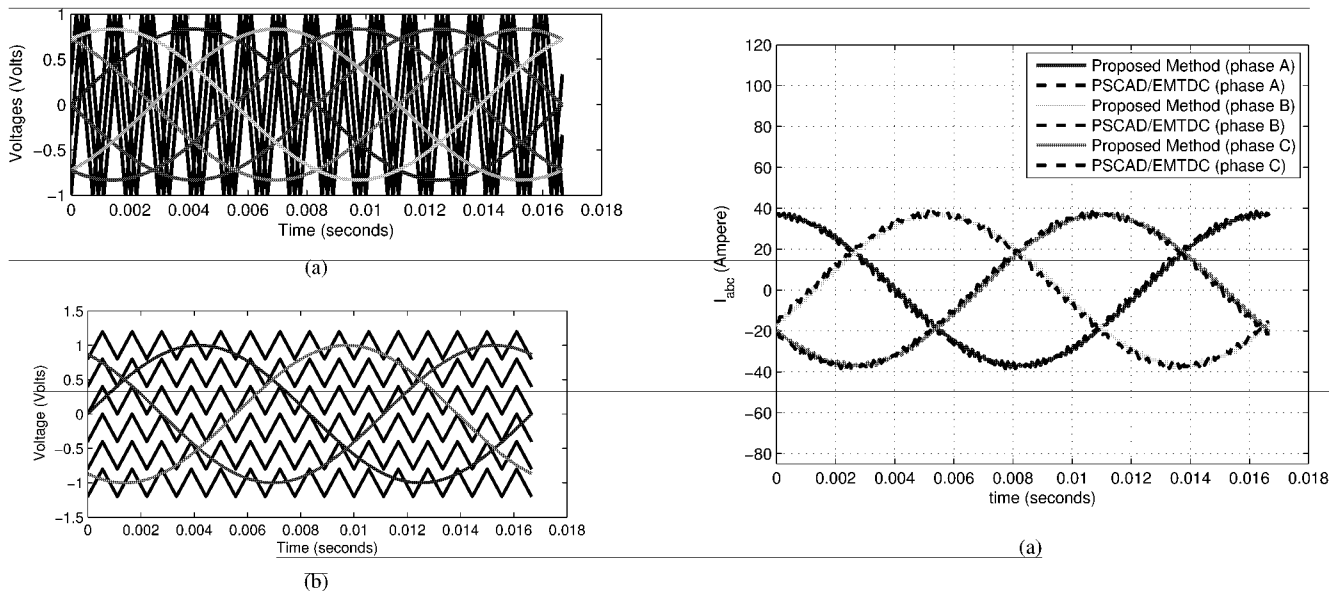


Fig. 2. Multicarrier Modulation Techniques: (a) PS-PWM Modulation; (b) IPD-PWM Modulation

TABLE I  
TABLE OF PARAMETER LIST

Parameter	Value	Parameter	Value
$R_a, R_b, R_c$	$0.02 \Omega$	firing angle, $\delta$	$0^\circ$
$L_a, L_b, L_c$	$0.0012 \text{ H}$	modulation index, $m_a$	$0.833$
$f$	$60 \text{ Hz}$	line-to-line voltage, $v_{sab}$	$200 \text{ V}$
$m_f$	$15$	carrier signal, $v_{er}$	$0.2 \text{ V}$
$v_{dca1}, v_{dca2}, v_{dca3}$	$72 \text{ V}$		
$v_{dcb1}, v_{dcb2}, v_{dcb3}$	$72 \text{ V}$		
$v_{dcc1}, v_{dcc2}, v_{dcc3}$	$72 \text{ V}$		

The steady-state current waveforms obtained by PSCAD/EMTDC and the proposed method for PS-PWM and IPD-PWM are shown in Fig. 3. The computation times of the proposed method is about two times shorter than those of PSCAD/EMTDC and S & S method. Moreover, the proposed method is more than 3 and 1.5 times faster than the PA method and Matlab expm function, respectively. Note that the proposed method is written in Matlab and, all its results are generated from uncompiled Matlab script files.

### B. Case 2: Unbalanced Condition

A 5% negative sequence voltage is superimposed on the system voltage to study operation under unbalanced condition. The system voltage is given by

$$\begin{aligned}
 v_{sa}(t) &= v_s \cos(\omega t) + 0.05v_s \cos(\omega t) \\
 v_{sb}(t) &= v_s \cos\left(\omega t - \frac{2\pi}{3}\right) + 0.05v_s \cos\left(\omega t + \frac{2\pi}{3}\right) \\
 v_{sc}(t) &= v_s \cos\left(\omega t + \frac{2\pi}{3}\right) + 0.05v_s \cos\left(\omega t - \frac{2\pi}{3}\right),
 \end{aligned}$$

Fig. 4 shows the resulting AC current waveforms obtained by PSCAD/EMTDC and the proposed method for PS-PWM and IPD-PWM. Moreover, due to the converter modulation operation, the dc current is expected to contain harmonics

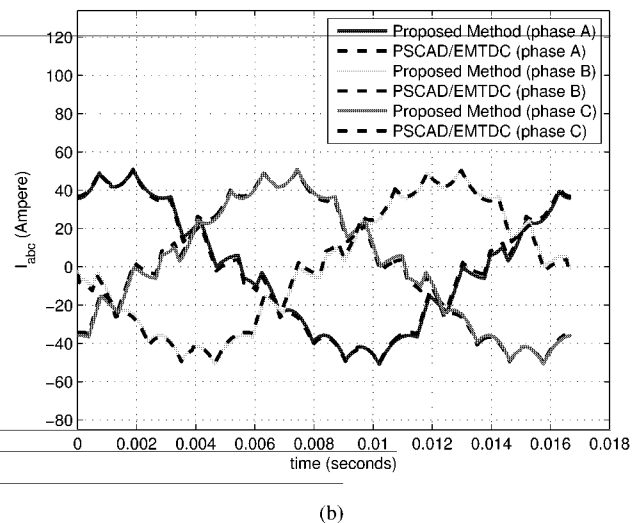
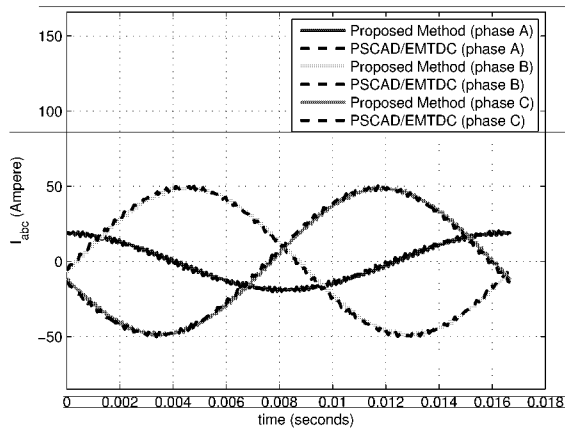


Fig. 3. AC current waveform at steady-state for Case 1: (a) PS-PWM Modulation; (b) IPD-PWM Modulation

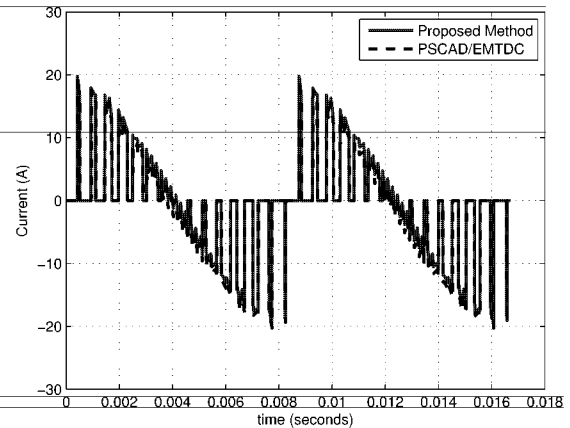
other than the second harmonics. Fig. 5 shows the dc current waveforms ( $I_{dc1}$  in Fig. 1) for PS-PWM and IPD-PWM. The results are in good agreement with those obtained by PSCAD/EMTDC. The waveform indicate that harmonics other than the second harmonics are also significant.

## VI. CONCLUSION

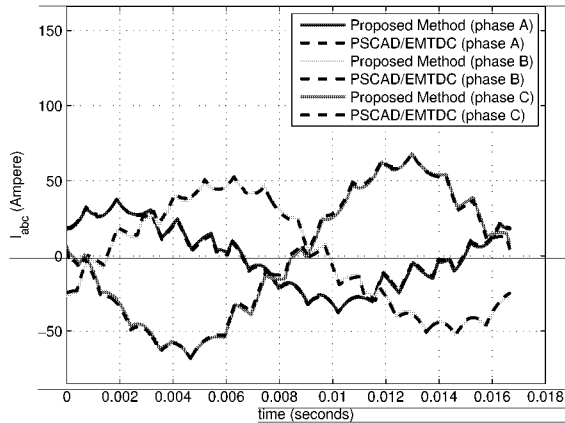
A new time-domain method based on Krylov subspace approach for calculating ac/dc current and voltage harmonics of a CHC is presented in the paper. The method is highly efficient. The computation time of the proposed method is about two times shorter than those of PSCAD/EMTDC and 1.5 times shorter than the solution provided by the Matlab expm function. All the results of the case studies obtained by the proposed method are consistent with those of PSCAD/EMTDC, demonstrating the validity of the method.



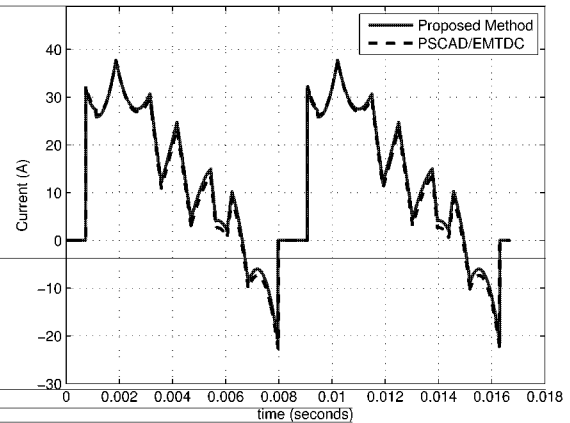
(a)



(a)



(b)



(b)

Fig. 4. AC current waveform at steady-state for Case 2: (a) PS-PWM Modulation; (b) IPD-PWM Modulation

Fig. 5. Current waveform of  $I_{dc1}$  for Case 2: (a) PS-PWM Modulation; (b) IPD-PWM Modulation

## VII. ACKNOWLEDGEMENT

The work is financially supported by the Ministry of Science and Technology under grant No. MOST105-2221-E-011-093-.

## REFERENCES

- [1] M. Angulo, P. Lezana, S. Kouro, J. Rodríguez, and B. Wu, "Level-shifted pwm for cascaded multilevel inverters with even power distribution," in *Power Electronics Specialists Conference*, 2007, pp. 2373–2378.
- [2] P. Lehn and K. L. Lian, "Frequency coupling matrix of a voltage-source converter derived from piecewise linear differential equations," *IEEE Transactions on Power Delivery*, vol. 22, no. 3, pp. 1603–1612, 2007.
- [3] I. M. Jaimoukha and E. M. Kasenally, "Krylov subspace methods for solving large lyapunov equations," *SIAM Journal on Numerical Analysis*, vol. 31, no. 1, pp. 227 – 251, 1994.
- [4] R. K. Subroto and K. L. Lian, "Modeling of a multilevel voltage source converter using the fast time-domain method," *IEEE Journal of Emerging and Selected Topics in Power Electronics*, vol. 2, no. 4, pp. 1117–1126, Dec 2014.
- [5] C. Moler and C. Van Loan, "Nineteen dubious ways to compute the exponential of a matrix, twenty-five years later," *SIAM Review*, vol. 45, no. 1, pp. 3 – 49, 2003.
- [6] K. Lian, "Derivation of a small-signal harmonic model for closed-loop power converters based on the state-variable sensitivity method," *IEEE Transactions on Circuits and Systems I: Regular Papers*, vol. 59, no. 4, pp. 833–845, 2012.
- [7] A. Semlyen, "Fundamental concepts of a krylov subspace power flow methodology," *IEEE Transactions on Power Systems*, vol. 11, no. 3, pp. 1528–1537, 1996.
- [8] Y. Saad, "Analysis of some krylov subspace approximations to the matrix exponential operator," *SIAM Journal on Numerical Analysis*, vol. 29, no. 1, pp. 209 – 228, 1992.
- [9] M. Bellalij, Y. Saad, and H. Sadok, "Further analysis of the arnoldi process for eigenvalue problems," *SIAM Journal on Numerical Analysis*, vol. 48, no. 2, pp. 393 – 407, 2010.
- [10] B. Wu, *High-Power Converters and AC Drives*. New Jersey, USA: Wiley, 2006.
- [11] S. Kouro, M. Malinowski, K. Gopakumar, J. Pou, L. Franquelo, B. Wu, J. Rodríguez, M. Perez, and J. Leon, "Recent advances and industrial applications of multilevel converters," *IEEE Transactions on Industrial Electronics*, vol. 57, no. 8, pp. 2553–2580, 2010.
- [12] G. Carrara, S. Gardella, M. Marchesoni, R. Salutari, and G. Sciutto, "A new multilevel pwm method: a theoretical analysis," *IEEE Transactions on Power Electronics*, vol. 7, no. 3, pp. 497–505, 1992.
- [13] N. Mohan, T. Undeland, and W. Robbins, *Power Electronics: Converters, Applications and Design*. New Jersey, USA: Wiley, 1995.
- [14] L. Maharjan, T. Yamagishi, H. Akagi, and J. Asakura, "Fault-tolerant operation of a battery-energy-storage system based on a multilevel cascade pwm converter with star configuration," *IEEE Transactions on Power Electronics*, vol. 25, no. 9, pp. 2386–2396, 2010.